Published in final edited form as:

Neurobiol Dis. 2019 July ; 127: 210–222. doi:10.1016/j.nbd.2019.02.022.

Impaired development of neocortical circuits contributes to the neurological alterations in *DYRK1A* haploinsufficiency syndrome

Juan Arranz[a,b,1,#], **Elisa Balducci**[a,b,#], **Krisztina Arató**[b,c,#], **Gentzane Sánchez-Elexpuru**[b,d,2], **Sònia Najas**[a,3], **Alberto Parras**[e], **Elena Rebollo**[a], **Isabel Pijuan**[a,b], **Ionas Erb**[c], **Gaetano Verde**[c,4], **Ignasi Sahun**[f], **Maria J. Barallobre**[a,b], **José J. Lucas**[e,g], **Marina P. Sánchez**[b,d], **Susana de la Luna**[b,c,h,i,*], **Maria L. Arbonés**[a,b,*]

[a]Instituto de Biología Molecular de Barcelona (IBMB), CSIC, 08028-Barcelona, Spain.

[b]Centro de Investigación Biomédica en Red de Enfermedades Raras (CIBERER), Barcelona, Spain.

[c]Centre for Genomic Regulation (CRG), The Barcelona Institute for Science and Technology (BIST), 08003-Barcelona, Spain.

[d]Department of Neuroscience, Laboratory of Neurology, IIS-Jiménez Díaz Foundation, 28040-Madrid, Spain.

[e]Department of Molecular Neuropathology, Centro de Biología Molecular Severo Ochoa (CBMSO), CSIC/UAM, 28049-Madrid, Spain.

[f]PCB-PRBB Animal Facility Alliance, 08020-Barcelona, Spain.

[g]Centro de Investigación Biomédica en Red de Enfermedades Neurodegenerativas (CIBERNED), Madrid, Spain.

[h]Universitat Pompeu Fabra (UPF), 08003-Barcelona, Spain.

[i]Institució Catalana de Recerca i Estudis Avançats (ICREA), Barcelona, Spain.

Abstract

Autism spectrum disorders are early onset neurodevelopmental disorders characterized by deficits in social communication and restricted repetitive behaviors, yet they are quite heterogeneous in terms of their genetic basis and phenotypic manifestations. Recently, *de novo* pathogenic

[*]Co-corresponding authors: M. L. Arbonés, IBMB, Barcelona Scientific Parc, Baldiri Reixac 4-8, 08028-Barcelona, Spain. Tel: +34 934033728; Fax: +34 934034979; marbmc@ibmb.csic.es, and S. de la Luna, CRG, Dr Aiguader 88, 08003-Barcelona, Spain. Tel: +34 933160144; Fax: +34 933160099; susana.luna@crg.eu.

[#]These authors contributed equally to the work.

[*]co-senior authors.

[1]Present address is: Institut D'Investigacions Biomèdiques August Pi i Sunyer (IDIBAPS), Barcelona, Spain.

[2]Present address is: Cambridge Institute for medical Research, University of Cambridge, Cambridge, UK.

[3]Present address is: Institute of Stem Cell Research, Helmholtz Zentrum München, German Research Center for Environmental Health (GmbH), Neuherberg, Germany.

[4]Present address is: Faculty of Medicine and Health Sciences, Universitat Internacional de Catalunya, Barcelona, Spain.

Conflict of Interest statement. None declared.

mutations in *DYRK1A*, a chromosome 21 gene associated to neuropathological traits of Down syndrome, have been identified in patients presenting a recognizable syndrome included in the autism spectrum. These mutations produce DYRK1A kinases with partial or complete absence of the catalytic domain, or they represent missense mutations located within this domain. Here, we undertook an extensive biochemical characterization of the *DYRK1A* missense mutations reported to date and show that most of them, but not all, result in enzymatically dead DYRK1A proteins. We also show that haploinsufficient *Dyrk1a*$^{+/-}$ mutant mice mirror the neurological traits associated with the human pathology, such as defective social interactions, stereotypic behaviors and epileptic activity. These mutant mice present altered proportions of excitatory and inhibitory neocortical neurons and synapses. Moreover, we provide evidence that alterations in the production of cortical excitatory neurons are contributing to these defects. Indeed, by the end of the neurogenic period, the expression of developmental regulated genes involved in neuron differentiation and/or activity is altered. Therefore, our data indicate that altered neocortical neurogenesis could critically affect the formation of cortical circuits, thereby contributing to the neuropathological changes in *DYRK1A* haploinsufficiency syndrome.

Keywords

autism spectrum disorder; cerebral cortex; DYRK1A mutations; epilepsy; neurodevelopment; transcriptome

1. Introduction

Autism spectrum disorder (ASD) is a neurodevelopmental disorder characterized by social communication deficits and restricted repetitive behaviors (Lord and Bishop, 2015), and it is frequent associated with intellectual disability (ID), language deficits and seizures (Geschwind, 2009; Sztainberg and Zoghbi, 2016). The causes of ASD remain largely unknown, although a genetic cause has been identified in around 25% of cases (Huguet et al., 2013). These genetic alterations include chromosomal rearrangements, *de novo* copy-number variants and *de novo* mutations in the coding-sequence of genes associated with chromatin remodeling, mRNA translation or synaptic function (de la Torre-Ubieta et al., 2016). Additionally, alterations in the production or migration of neocortical neurons are a point of convergence for ASD and ID (de la Torre-Ubieta et al., 2016; Ernst, 2016; Packer, 2016).

DYRK1A is a member of the conserved dual-specificity tyrosine-regulated kinase (DYRK) family of protein kinases (Aranda et al., 2011) that has different functions in the nervous system (Tejedor and Hammerle, 2011). This kinase influences brain growth, an activity that is conserved across evolution (Fotaki et al., 2002; Kim et al., 2017; Tejedor et al., 1995). *DYRK1A* is located within the Down syndrome (DS) critical region on human chromosome 21 (Guimera et al., 1996). There is evidence that triplication of the gene contributes to neurogenic cortical defects (Najas et al., 2015) and other neurological deficits in DS, making it a potential drug target for DS-associated neuropathologies (Becker et al., 2014). Recently, mutations in *DYRK1A* have been identified in a recognizable syndromic disorder named *DYRK1A* haploinsufficiency syndrome (DHS), also known as MRD7 (Mental Retardation

Autosomal Dominant 7; OMIM: 614104) and DYRK1A-related intellectual disability syndrome (ORPHANET: 464306, 464311 and 268261). ASD-related deficits are common clinical manifestations in DHS, which include moderate to severe ID, intrauterine growth retardation, developmental delay, microcephaly, seizures, speech problems, motor gait disturbances and a dysmorphic *facies* (Earl et al., 2017; Luco et al., 2016; van Bon et al., 2016). The mutations identified to date in patients with DHS are *de novo*, involving chromosomal rearrangements (Courcet et al., 2012; Moller et al., 2008; van Bon et al., 2011), small insertions or deletions, and nonsense mutations (Courcet et al., 2012; Earl et al., 2017; O'Roak et al., 2012; van Bon et al., 2016) and references therein). These mutations lead to the production of truncated DYRK1A proteins that lack partially o totally the kinase domain and that are therefore catalytically inactive. *DYRK1A* missense mutations have also been identified in patients with a distinctive DHS phenotype (Bronicki et al., 2015; Dang et al., 2018; De Rubeis et al., 2014; Deciphering Developmental Disorders, 2015; Evers et al., 2017; Ji et al., 2015; Ruaud et al., 2015; Stessman et al., 2017; Trujillano et al., 2017; Wang et al., 2016; Zhang et al., 2015). The structural modeling of these mutations predicts that they are loss-of-function (LoF) mutations (Evers et al., 2017; Ji et al., 2015). However, experimental data supporting this prediction have been reported only for a few of them (Widowati et al., 2018).

The *Dyrk1a*$^{+/-}$ mouse displays some of the core traits of DHS, including developmental delay, microcephaly, gait disturbances and learning problems (Arque et al., 2008; Fotaki et al., 2002; Fotaki et al., 2004). The cell density in the neocortex of the adult mutant mouse is altered (Fotaki et al., 2002; Guedj et al., 2012) but the origin of this alteration and the neuronal components affected are unknown. To gain additional insight into the pathogenesis of DHS, we have performed a biochemical study to assess the impact of all reported missense mutations within the catalytic domain on *DYRK1A* activity. Furthermore, we analyzed the cytoarchitecture and gene expression profile of the neocortex in *Dyrk1a*$^{+/-}$ mice, also performing behavioral tests and obtaining electroencephalogram (EEG) recordings from these animals. Our results indicate that defects in the production of excitatory neocortical neurons are critical to the neuropathology of DHS.

2. Materials and methods

2.1. Plasmids

The plasmids to express HA-tagged DYRK1A have been described previously (Alvarez et al., 2003): human isoform 754 aa; NP_569120; wild type (WT); or a kinase inactive version in which the ATP binding lysine 179 (K188R in the 763 aa isoform) was replaced by arginine. Single nucleotide mutations (numbering based on the 763 aa isoform, as appears in most publications: Supplementary Table 1 and Fig. 1A) were introduced into the HA-DYRK1A expression plasmid using the QuickChange Multi Site-Directed Mutagenesis Kit, according to the manufacturer’s instructions (Agilent Technologies) and with primers specific to each mutant (Supplementary Table 2). The A469fs* and A489fs* mutations were produced by a T or C deletion, respectively, and the same alterations were created in the DYRK1A expression plasmid. The plasmids generated by site-directed mutagenesis were

verified by DNA sequencing and the transfection efficiency was assessed by co-transfection with a green fluorescent protein (GFP) expression plasmid (pEGFP-C1, Clontech).

2.2. Animals

We used embryos and postnatal and adult *Dyrk1a*$^{+/-}$ mice and their control *Dyrk1a*$^{+/+}$ littermates, generated and genotyped as described elsewhere (Fotaki et al., 2002; Najas et al., 2015). The day of the vaginal plug was defined as E0 and the day of birth was defined as P0. After weaning, mice from the same litter and of the same gender were housed in groups. The animals were maintained at the PCB-PRBB Animal Facility in ventilated cages on a 12 h light/dark cycle, at approximately 20°C and in 60% humidity, and with food and water supplied *ad libitum*. For bromodeoxyuridine (BrdU) birthdating experiments, pregnant females were peritoneally injected with a BrdU solution (50 mg/kg; Sigma), two injections spaced 4 h, and pups were collected and processed at P7. Experimental procedures were carried out in accordance with the European Union guidelines (Directive 2010/63/EU) and the protocols were approved by the Ethics Committee of the CSIC, PCB-PRBB, CBM and Fundación Jiménez Díaz.

2.3. Cell culture and transfection

The HEK293T cell line was obtained from the American Type Culture Collection (www.atcc.org) and used for the exogenous expression of DYRK1A mutants. The cells were maintained at 37°C in Dulbecco's modified Eagle medium (DMEM; Invitrogen), with 10% fetal bovine serum (FBS; Invitrogen) and supplemented with antibiotics (100 μg/ml penicillin and 100 μg/ml streptomycin; Invitrogen). The cells were transfected by the calcium phosphate precipitation method and processed 48 h after transfection.

2.4. *In vitro* kinase (IVK) assays

Cells were washed in phosphate buffered saline (PBS) and then lysed in HEPES lysis buffer (50 mM Hepes [pH 7.4], 150 mM NaCl, 2 mM EDTA, 1% NP-40) supplemented with a protease inhibitor cocktail (#11836170001, Roche Life Science), 30 mM sodium pyrophosphate, 25 mM NaF and 2 mM sodium orthovanadate. The lysates were cleared by centrifugation and incubated overnight at 4°C with protein G-conjugated magnetic beads (Dynabeads, Invitrogen) previously bound to an antibody against HA (Covance, #MMS-101R). The beads were then washed 3 times with HEPES lysis buffer and used for either IVK assays or to probe Western blots to control for the presence of HA-tagged DYRK1A. For the IVK assays, immunocomplexes were washed in kinase buffer (25 mM HEPES [pH 7.4], 5 mM $MgCl_2$, 5 mM $MnCl_2$, 0.5 mM DTT) and further incubated for 20 min at 30°C in 20 μl of kinase buffer containing 50 μM ATP, [γ^{32}P]-ATP (2.5×10^{-3} μCi/pmol) and with 200 μM DYRKtide as the substrate peptide. The incorporation of ^{32}P was determined in triplicates as described previously (Himpel et al., 2000), and the kinase activity was normalized to the amount of DYRK1A protein present in the immunocomplexes determined in Western blots (see Supplementary Materials and Methods for details and Table 3 for information on primary antibodies). DYRK1A autophosphorylation was analyzed by SDS-PAGE fractionation of the immunocomplexes and exposure of the dried gel to film.

2.5. RNA extraction, microarray analysis and RT-qPCR

Postnatal day (P) 0 and P7 *Dyrk1a*$^{+/+}$ and *Dyrk1a*$^{+/-}$ mice (4-9 animals each condition) were sacrificed by decapitation and the brain cortices were dissected out and stored at −80°C. The tissue samples were homogenized in a Polytron and the total RNA was extracted with the TriPure Isolation Reagent (Roche). A RNA clean-up step was performed using the RNeasy Mini Kit (Qiagen) followed by DNAse I treatment (Ambion). Only RNA samples with an integrity number above 8.0 (Agilent 2001 Bioanalyzer) were used for further analysis. For microarray studies, total RNA was hybridized to an Affymetrix Mouse GeneChip 430 2.0 Array. RNA was analyzed by reverse transcription coupled to quantitative PCR (the sequence of the qPCR primers is found in Supplementary Table 4) or using a low-density array (probes included in Supplementary Table 5). For more detailed information see Supplementary Materials and Methods. The microarray data reported in this paper has been submitted to the GEO repository with accession number GSE127707.

2.6. Video-EEG recordings

Video-EEG recordings of adult *Dyrk1a*$^{+/+}$ and *Dyrk1a*$^{+/-}$ male mice (8 animals each genotype) aged 5-6 months were obtained as described elsewhere (Garcia-Cabrero et al., 2012). Two home-made EEG stainless steel electrodes were implanted symmetrically into an anesthetized mouse over the cortex in front of bregma, and the ground and reference electrodes were placed posterior to lambda (Fig. 2C). A plastic pedestal (Plastic One Inc., Roanoke, VA, USA) was used to attach the pins of the electrodes, and the headset was fixed to the skull and the wound closed with dental cement (Selectaplus CN, Dentsply DeTrey GmbH, Dreireich, Germany). Four days after surgery, synchronized video-EEG activity was recorded for 48 h in freely moving mice using a computer-based system (Natus Neurowork EEG, Natus Medical Inc., San Carlos, CA, USA). EEG seizure activity was examined by inspecting the entire EEG records and behavioral correlations were reviewed within the corresponding video-type segments.

2.7. Behavioral Tests

The social and stereotyped behaviors (social interaction and marble-burying tests) of adult 4-6 month old *Dyrk1a*$^{+/+}$ and *Dyrk1a*$^{+/-}$ male mice (12-15 animals each genotype) were tested in a dedicated room for behavioral studies during the light phase. Before the experiment, the animals were habituated to the room for at least 30 min and during the test, the mice were recorded from above with a video-camera CCTV (Sonny Corporation). The animal's behavior was analyzed by an observer blind to their genotype using the SMART 3.0 software (Panlab Harvard Apparatus). See Supplementary Materials and Methods for more details on these procedures as well as for the UsV analysis.

2.8. Tissue preparation, immunostaining, and cell and synapse counts

To obtain brain tissue, P7 and adult *Dyrk1a*$^{+/+}$ and *Dyrk1a*$^{+/-}$ mice (4-9 animals each condition) were deeply anesthetized and transcardially perfused with 4% paraformaldehyde. The mouse's brain was removed and post-fixed, and cryotome or vibratome brain sections were immunostained as described previously (Barallobre et al., 2014). To quantify neurons and synapses, images were obtained on a Leica AF6500 motorized wide-field microscope

and a Zeiss LSM780 confocal microscope, respectively. To quantify BrdU-labeled cells, images were obtained on an Olympus BX51 motorized microscope with a JVC digital color camera. The procedures for immunostaining, and cell and synapse quantification are indicated in the Supplementary Materials and Methods. The source of the primary antibodies for these procedures is indicated in Supplementary Table 6.

2.9. Statistical analysis

Statistical analyses were performed with GraphPad Prism v5.0a (GraphPad Software) or with SPSS (IBM Analytics Software). The data from the IVK studies were analyzed with a 2-tailed unpaired Mann-Whitney test, synapse counts with a nested one-way ANOVA test, and the rest of the analysis was performed with a two-tailed unpaired Student's *t*-test. Differences were considered significant at $p < 0.05$. In the histograms, the data are represented as the mean ± standard error of the mean (SEM).

3. Results

3.1. *DYRK1A* missense mutations in individuals with DYRK1A haploinsufficiency are loss-of-function mutations

The kinase activity associated with most of *DYRK1A* missense mutations has been inferred from their position within the DYRK1A catalytic domain (Evers et al., 2017). Given that experimental data supporting the predicted models have been reported very recently for only a few *DYRK1A* missense mutations (Widowati et al., 2018), we set out to analyze the kinase activity of all missense mutations within the DYRK1A catalytic domain published to date and some others included in the ClinVar database (www.ncbi.nlm.nih.gov/clinvar/?term=DYRK1A[gene]). We also included 2 missense mutations in the non-catalytic C-terminal region (R528W and T588N) and 3 mutations generating truncated proteins at the end of the kinase domain and predicted to contain the whole catalytic domain (Fig. 1A, Table 1 and Supplementary Table 1). These mutations were introduced into a DYRK1A expression plasmid and the catalytic activity of each of the mutants was evaluated using an IVK assay with the DYRKtide peptide as the substrate (see experimental design in Fig. 1B). The activity of most of the missense mutants was comparable to that of the DYRK1A K188R kinase-dead mutant (Fig. 1C), although the L295F, Q313H and R438H mutants rendered proteins with half the activity of the WT protein (Fig. 1C). However, some of the mutations did not alter the DYRK1A catalytic activity (K167R and T588N), and six even enhanced the enzyme's kinase activity: A195T, H223R, L259F, R458M, G486D and R528W (Fig. 1C). Notably, the activity of the truncated proteins increased with the length of the resulting protein, with truncations at R467 (before the α-helix I) devoid of activity, and at F478 (downstream α-helix I) with just 10% activity (Fig. 1C). Moreover, the fact that the A498Pfs93* mutant does not have similar catalytic activity to the WT protein might indicate that all or part of the non-catalytic C-terminal region is required for full DYRK1A kinase activity. Of note, the crystal structures of DYRK1A have been obtained with truncated proteins that, based on our data, are not fully active (Soundararajan et al., 2013).

Considering the mode of activation of DYRK1A (Lochhead et al., 2005), the negative results in the IVK assays could be due to defective autophosphorylation of the Tyr residue in the

activation loop, or to the inability of the mutants to phosphorylate an exogenous substrate. The lack of activity on the substrate was correlated with a lack of Tyr phosphorylation (Fig. 1D), suggesting that the mutations altered the activation of the kinase. We also evaluated the autophosphorylation of the mutant proteins (Fig. 1B), an activity associated with the mature kinase (Himpel et al., 2001), and only the catalytically active mutant enzymes were seen to autophosphorylate, with the exception of the truncated mutant A498Pfs93* (Fig. 1D and Supplementary Fig. 1A and B). In this latter case, either the autophosphorylation sites are located in the missing C-terminal region or the mutation alters the substrate preference of the protein. Together, these results indicate that most but not all of the missense DYRK1A mutants reported to date in DHS are *bona-fide* LoF mutants.

There is deficient accumulation of the kinase-dead DYRK1A K188R mutant (Kii et al., 2016) and therefore, we evaluated the quantitative expression of these mutants and their stability (Fig. 1E: stability index). We confirmed the reduced accumulation of the K188R mutant relative to the WT protein (Fig. 1F), and a similar behavior was observed for other catalytically inactive mutants (Fig. 1F and Supplementary Fig. 1C). In fact, kinase activity and protein stability were positively correlated (Fig. 1G), suggesting that in heterozygosis, the proteins expressed from the mutant allele will not accumulate as much as the WT protein, thereby reducing their potential dominant-negative activity.

3.2. Stereotyped behavior and epileptic activity of *Dyrk1a*$^{+/-}$ mice

Seizures, stereotypies and social anxiety are frequent in DHS (Earl et al., 2017; van Bon et al., 2016). The *Dyrk1a*$^{+/-}$ mouse is more sensitive to the convulsive agent pentylenetetrazol (Souchet et al., 2014) and it displays anxiety-like behavior in the open field (Fotaki et al., 2004), although ASD-like behaviors and epileptiform activity have not been reported in this model. Recently, a mouse carrying a frame-shift mutation in *Dyrk1a* has been generated and mice heterozygous for this mutation develop deficits in social contacts and communicative ultrasonic vocalization (UsV), as well as hyperthermia-induced seizures (Raveau et al., 2018). *Dyrk1a*$^{+/-}$ pups displayed similar deficits in UsV when separated from their mothers (Supplementary Fig. 2A). Moreover, adult *Dyrk1a*$^{+/-}$ mice engaged in shorter social olfactory interactions (oral-oral or oral-genital sniffing) in the resident-intruder test, while more time was spent on repetitive digging and self-grooming (Fig. 2A). Stereotyped behaviors were further evaluated in the marble-burying test, and the *Dyrk1a*$^{+/-}$ mutant mice buried fewer marbles and spent less time digging than their WT littermates (Fig. 2B and Supplementary Fig. 2B). Furthermore, *Dyrk1a*$^{+/-}$ mutants spent less time exploring the central region of the cage where the marbles were buried (*Dyrk1a*$^{+/+}$ 288±41 s, *Dyrk1a*$^{+/-}$ 133±15 s; $p < 0.001$, Student's *t*-test). This time difference is unlikely to be caused by less locomotor activity, as both genotypes entered the central region a similar number of times (*Dyrk1a*$^{+/+}$ 41±5, *Dyrk1a*$^{+/-}$ 35±4 s; $p < 0.314$, Student's *t*-test). Rather, *Dyrk1a*$^{+/-}$ mice spent significantly longer on repetitive self-grooming (Fig. 2B). Together, these results show that in addition to deficits in social communication, haploinsufficient *Dyrk1a*$^{+/-}$ mice develop repetitive and stereotyped behaviors.

The epileptic activity in *Dyrk1a*$^{+/-}$ mice was evaluated from video-EGG recordings (Fig. 2C-H), which revealed differences in the basal activity between the distinct genotypes

(*Dyrk1a*$^{+/+}$ 9-12 Hz; *Dyrk1a*$^{+/-}$ 6-7 Hz: Fig. 2D). Spontaneous myoclonic jerks that corresponded to interictal epileptiform activity were evident in *Dyrk1a*$^{+/-}$ mice, with isolated spikes, polyspikes and spike-wave discharges (Fig. 2E-G). These mutant mice also experienced periods of immobility, during which grooming, feeding and exploration were suppressed. Such periods of inactivity, alternating with shorter ones of epileptic activity, were characterized by groups of spikes and polyspikes in the EEG recordings (Fig. 2E and F). At times, the epileptic activity in *Dyrk1a*$^{+/-}$ mice coincided with situations of moderate handling stress. In half of the *Dyrk1a*$^{+/-}$ mice (4 out of 8), spontaneous generalized tonic-clonic seizures were recorded that lasted for different periods, with distinct lengths of tonic and clonic phases, and motor correlates that corresponded to stage 5-6 in the modified Racine Scale (Luttjohann et al., 2009); see Fig. 2H and Supplementary Movie). Notably, about half of the patients with mutations in *DYRK1A* develop epilepsy, displaying atonic attacks, absences and generalized myoclonic seizures (van Bon et al., 2016). Thus, epileptic activity seems to be a common characteristic in humans and mice with DHS.

3.3. Alterations in neuron numbers in the developing neocortex of *Dyrk1a*$^{+/-}$ mice

The neocortex is a six-layered structure essential for higher cognitive functions and sensory perception. Most neocortical neurons (more than 80% in the mouse) are projection excitatory neurons that extend their axons to intracortical or subcortical targets and use glutamate as neurotransmitter. The distinct types of excitatory neurons are produced in the embryo dorsal telencephalon (from E11.5 to E17.5 in the mouse) in overlapping temporal waves. The first neurons formed are those that are closest to the ventricle (layer VI neurons) and the last formed are those neurons located in the most superficial layers (layers II-III neurons) (Florio and Huttner, 2014; Molyneaux et al., 2007). Of note, perturbations in sensory regions and in the circuits that connect these regions have been described in several ASD mouse models (Golden et al., 2018). We previously showed that production of the early-born cortical neurons is enhanced in *Dyrk1a*$^{+/-}$ embryos (Najas et al., 2015). To obtain further evidence as to how *Dyrk1a* haploinsufficiency affects cortical development, we counted the number of neurons that express the neuronal marker NeuN in the internal (V-VI) and external (II-IV) layers of the somatosensory cortex (SSC) at P7 (Fig. 3A), when radial migration has ended and excitatory neurons adopt their final positions (Miller, 1995). The neocortical layers were thinner in postnatal *Dyrk1a*$^{+/-}$ mice, while they contained more neurons than their *Dyrk1a*$^{+/+}$ littermates (Fig. 3B and C). The fact that the neuronal densities in the internal and external layers of *Dyrk1a*$^{+/-}$ mutants are similarly affected (Fig. 3C) suggests that *Dyrk1a* haploinsufficiency may alter neuron production along the neurogenic phase of cortical development. This possibility was evaluated with BrdU-birthdating analysis (Fig. 3D-F). The results showed that P7 *Dyrk1a*$^{+/-}$ animals had more BrdU^{+} cells in the SSC than WT animals when the BrdU labeling was performed at E13.5 (Fig. 3D), indicating that neurogenesis is enhanced in the *Dyrk1a*$^{+/-}$ mutant at this developmental stage. By contrast, *Dyrk1a*$^{+/+}$ and *Dyrk1a*$^{+/-}$ animals displayed similar numbers of BrdU^{+} cells when the treatment was performed at E15.5 (Fig. 3F). Additional BrdU-labeling experiments indicated that cortical neurogenesis in *Dyrk1a*$^{+/-}$ embryos ends at the correct time (Supplementary Fig. 4). Consistent with the temporal generation of cortical excitatory neurons (Molyneaux et al., 2007), the BrdU-labeled cells generated at E15.5 were concentrated in the external layers of P7 WT animals, while the labeled cells generated at

E13.5 showed a broader layer distribution, with $BrdU^+$ cells located in both internal and external layers (Fig. 3E and G). Additionally, the distribution of BrdU-labeled cells in *Dyrk1a*$^{+/-}$ animals was similar to that in WT animals (Fig. 3E and G), indicating that radial migration of excitatory neurons is not affected in the *Dyrk1a*$^{+/-}$ model. Taking all the results together, we conclude that the augmented neuron density in the neocortex of *Dyrk1a*$^{+/-}$ mutants is the result of an increased neuron production during early and mid-corticogenesis.

Finally, the differentiation of excitatory neurons was assessed by studying the layer-specific markers Ctip2 (layer V) and Mef2c (layers II-IV). *Dyrk1a*$^{+/-}$ mutants have fewer $Ctip2^+$ neurons and more $Mef2c^+$ neurons than their WT littermates (Fig. 3B and C). As the distinct types of neocortical excitatory neurons display different electrophysiological properties and project to distinct target areas (Molyneaux et al., 2007), the alteration in the proportions of these neurons could modify the final wiring of the brain in the *Dyrk1a*$^{+/-}$ mutants.

3.4. Alterations to the synaptic circuitry in the neocortex of adult *Dyrk1a*$^{+/-}$ mice

Around 10-15% of neocortical neurons are interneurons that make local connections and use γ-aminobutyric acid (GABA) as a neurotransmitter (Markram et al., 2004). These neurons maintain the stability of cortical networks and they modulate network activity through synaptic inhibition (Somogyi et al., 1998). In fact, disturbances to the excitation/inhibition ratio (E/I imbalance) in relevant brain circuits have been proposed as a common pathogenic mechanism in ASD (Rubenstein, 2010). Studies in ASD mouse models indicate that E/I imbalance may arise not only from changes in synapse function and homeostasis but also from an altered proportion of excitatory and inhibitory neurons (de la Torre-Ubieta et al., 2016).

We have previously shown that the brain of adult *Dyrk1a*$^{+/-}$ mice present altered levels of proteins related to the glutamatergic and GABAergic systems (Souchet et al., 2014). Based on these data, we wondered whether the defects in cortical development displayed by the *Dyrk1a*$^{+/-}$ mice results in alterations in the adult circuitry. To this aim, we analyzed the excitatory ($NeuN^+/GABA^-$) and inhibitory ($GABA^+$) neurons in the SSC of adult animals (Fig. 4A and B). The number of excitatory neurons in *Dyrk1a*$^{+/-}$ mutants increased in both the internal and external neocortical layers. The heterozygous mice also had more GABAergic neurons than their WT littermates, although the difference between these genotypes was only significant in the internal layers (Fig. 4B). The density of excitatory and inhibitory synapses was estimated in adult neocortices using antibodies against presynaptic markers VgluT1 (vesicular glutamate transporter 1) or VGAT (vesicular GABA transporter), and the postsynaptic markers Homer or Gephyrin. There was a significant increase in excitatory synapses in *Dyrk1a*$^{+/-}$ mutants in the two layers examined (IV and VI), while the density of inhibitory synapses in the mutant mice was similar to that in WT animals (Fig. 4C and D). The alterations in the proportion of glutamatergic and GABAergic neurons and synapses observed in the *Dyrk1a*$^{+/-}$ neocortices may contribute to the ASD-related behavior and epileptic activity in these animals.

3.5. Transcriptome alterations in the postnatal *Dyrk1a*$^{+/-}$ cerebral cortex

The amount of Dyrk1a protein in the mouse developing neocortex increases during neurogenesis, reaching maximum levels in late embryonic development and during the first postnatal week (Dang et al., 2018). At these developmental stages, neural precursors shift their status and become gliogenic (Kriegstein and Alvarez-Buylla, 2009), while neurons extend neurites and synaptogenesis begins (Li et al., 2010). These processes are coordinated by transcriptional programs that are dynamically regulated during development (Telley et al., 2016), and it is possible that alterations to these programs might contribute to the early neurological phenotype in *Dyrk1a* haploinsufficiency. To test this possibility, we compared the transcriptional profile of the cerebral cortex in *Dyrk1a*$^{+/+}$ and *Dyrk1a*$^{+/-}$ mice at P0 and P7 (Supplementary Fig. 6A for the microarray experimental design and Fig. 5A for the comparisons performed). The comparison of the Dyrk1a expression profile during cortical development in *Dyrk1a*$^{+/+}$ and *Dyrk1a*$^{+/-}$ mice confirmed that *Dyrk1a* expression was reduced by half in the cortices of *Dyrk1a*$^{+/-}$ mice at any time-point, reflecting *Dyrk1a* haploinsufficiency (Supplementary Fig. 5).

The heatmap representation of the microarray expression data showed that the developmental effect on gene expression was more relevant than the effect of the reduction in *Dyrk1a* dose (Supplementary Fig. 6B). In fact, the analysis of genes differentially expressed between P7 and P0 in *Dyrk1a*$^{+/-}$ cortex showed numbers similar to the WT samples (Fig. 5B; see also Supplementary Fig. 7 for validation of the microarray results and Supplementary Dataset 1). A large proportion of the genes that were differentially expressed during development in the WT samples changed in the same direction in *Dyrk1a* mutant samples (Supplementary Fig. 6B). However, the expression of many of the genes that were up-regulated during development in the WT samples was diminished in *Dyrk1a*$^{+/-}$ samples and *vice versa* (Fig. 5C). These results suggest that *Dyrk1a* haploinsufficiency does not have a strong impact on the transcriptional program that drives postnatal cortical development but rather, that it might affect the time-course of the repression/activation of transcription. Nevertheless, the expression of a subset of genes was significantly altered between the two genotypes at P0 (182 genes) or P7 (73 genes), with changes greater or less than 1.4 fold (Fig. 5D).

Pathway enrichment analysis of the genes differentially expressed when comparing P0 and P7 WT cortices showed that the up-regulated genes at P7 were associated with synaptic transmission, while the down-regulated ones were enriched in cell cycle-associated functions (Supplementary Fig. 8). These data are consistent with the developmental changes occurring in the neocortex, since differentiating neurons acquire terminal features. Indeed, at these stages most pluripotent progenitors in the ventricular zone lose their capacity to self-renew or become less proliferative, producing cells of the glial lineage (Kriegstein and Alvarez-Buylla, 2009). When analyzing the genes with transcriptional changes in the *Dyrk1a*$^{+/-}$ samples compared to the WT ones, no particular enrichment was associated with the up-regulated genes in the *Dyrk1a*$^{+/-}$ animals, although known regulators of gliogenesis were identified in this set, such as *Sox4* or *Sox11* (Fig. 5E), suggesting a possible defect in the onset of glial cell production in the *Dyrk1a*$^{+/-}$ mutant model. By contrast, the down-regulated set was enriched in genes whose products are located in dendrites (*Calb1, Penk,*

Thy1) and/or that are involved in axon growth (*Nefl, Nefm*) or synaptic transmission (*Gabral, Gabrg1, Htr7*: Fig. 5E and Supplementary Dataset 2). Hence, the transcriptional alterations detected further support that neuron activity is altered in the neocortex of *Dyrk1a* $^{+/-}$ mutant pups.

4. Discussion

In this study, we analyzed a series of *DYRK1A* missense mutations, most of which are *bona-fide* LoF mutants that render the DYRK1A proteins enzymatically inactive. Moreover, the positive correlation between activity and protein accumulation might indicate that the presence of kinase-dead proteins has an added harmful effect. Very recently, the analysis of several DYRK1A missense mutants found in humans has been published, with a focus on the biochemical properties of the kinase variants (Widowati et al., 2018). Some of these variants are included in our analysis (for instance, L245R, D287N and T588N), and results are in agreement regarding the effect of the mutations on the DYRK1A catalytic activity. Our work further expands this analysis by including all missense mutations in the catalytic domain of DYRK1A published to date. Some of these mutations lie in regions predicted to be essential, as the case of K188 in the ATP-binding domain or D287 and F308 (HCD- and DFG-motifs, respectively), which are involved in the catalytic reaction. There is a particular accumulation of mutations within the P+1 loop and the α-helix F (R325H, Y327C, R328W, S346F/P, L347R), which render catalytically inactive kinase proteins. In addition, though the number of missense mutations is still low, some residues can be considered as hot spots either because the mutation has been reported in two different patients (S346P: (Bronicki et al., 2015; Deciphering Developmental Disorders, 2015); R467Q: (Evers et al., 2017; Posey et al., 2016)) and/or because the same residue is mutated to different amino acids (D287V and D287Y: (Deciphering Developmental Disorders, 2015; Zhang et al., 2015); S346P and S346F: (Bronicki et al., 2015) and ClinVar SCV000712522). All of the mutations resulting in kinases without catalytic activity are present in individuals with clinical traits associated to the DHS; likewise, individuals with mutations leading to kinases with partial activity (L295F, Q313H and tA498Pfs93*) present DHS features (Table 1 and Supplementary Table 1), suggesting that there is a threshold for DYRK1A activity regarding non pathological phenotypes.

Somewhat unexpectedly, the enzymatic activity of several missense mutants was indistinguishable from that of the WT kinase (K167R, T588N) and in some cases, even an increment in activity was detected (A195T, H223R, L259F and R458M). No clinical information is available for some of these variants and therefore, no correlations can be established. For others, as the case of A195T, we cannot exclude that the activity of the mutants could be the reflection of an altered substrate choice; alternatively, they might lead to other alterations in DYRK1A function affecting its final biological activity with pathological consequences. A third possibility could be that they represent pathogenic variants of DYRK1A hyperactivity, based on the links of DYRK1A overexpression with certain DS pathological traits (Becker et al., 2014). Of note, the hyperactive G486D mutation was identified in a patient with macrocephaly (Dang et al., 2018), in contrast with the DHS patients with LoF mutations in which microcephaly is, generally, observed (Table 1). Finally, the results might also mean that these mutations do not provoke any negative

effects. Indeed, the effects of the catalytic missense A195T and L259F mutants have been evaluated in cultured cortical neurons, where their impact on neurite extension was similar to that of the WT neurons (Dang et al., 2018). Therefore, in the case of the catalytically active mutants, the possibility that these genetic variants in the *DYRK1A* gene are not responsible for the clinical phenotype should also be considered.

In ASD and ID syndromes, alterations to dendrite morphogenesis and synapse formation are common (de la Torre-Ubieta et al., 2016). There is evidence that DYRK1A regulates the actin cytoskeleton and microtubule dynamics, thereby contributing to the development and maintenance of neurites and dendritic spines (Martinez de Lagran et al., 2012; Ori-McKenney et al., 2016; Park et al., 2012). Indeed, the morphology of the dendritic arbor in neurons of the motor cortex is altered in *Dyrk1a*$^{+/-}$ mice and in transgenic mice overexpressing *Dyrk1a* (Benavides-Piccione et al., 2005; Martinez de Lagran et al., 2012). These, together with the detrimental effect of *DYRK1A* truncated mutations in neuronal dendritic and spine growth (Dang et al., 2018) suggested that postnatal neocortical development is relevant to the neuropathology of DHS. However, our results indicate that *Dyrk1a* haploinsufficiency also affects neuron production in the developing neocortex leading to alterations to the number and proportion of the excitatory neuron subtypes. Considering that each of the many distinct excitatory neural subtypes fulfills a particular function (Jabaudon, 2017), subtle alterations in the proportion of these neurons would influence the activity of the synaptic circuits formed during postnatal development. In this context, the different transcriptomic profiles of the postnatal *Dyrk1a*$^{+/-}$ neocortex could be the consequence of its different neuronal composition. However, given that DYRK1A can directly or indirectly regulate transcription (Aranda et al., 2011; Di Vona et al., 2015), *Dyrk1a* haploinsufficiency might specifically modify the transcriptional programmes in differentiating neocortical neurons. In any case, the transcriptome analysis highlighted the weaker expression of genes involved in neuritogenesis and synaptic activity in the postnatal *Dyrk1a*$^{+/-}$ neocortex. Therefore, both the reduction in gene expression and the direct activity of DYRK1A on proteins implicated on neuritogenesis should be considered as factors that contribute to the neurological alterations in *Dyrk1a*$^{+/-}$ mutant mice.

Adult *Dyrk1a*$^{+/-}$ mice experience epileptic activity and behavior deficits similar to those observed in other ASD mouse models in which excitatory and/or inhibitory synaptic circuits are perturbed (Lee et al., 2017). In fact, altered production and/or migration of excitatory and/or inhibitory cortical neurons affects the E/I balance in mature circuits, usually making them epileptogenic (Bozzi et al., 2012; Rubenstein, 2010). *Dyrk1a*$^{+/-}$ mutants exhibit an excess of excitatory neurons and synapses in the neocortex, and these animals also show an excess of inhibitory neurons in the internal neocortical layers. Thus, we propose that both excitatory and inhibitory neurons contribute to the E/I imbalance underlying the epileptic activity, ASD-like behavior and cognitive deficits associated with DHS.

Supplementary Material

Refer to Web version on PubMed Central for supplementary material.

Acknowledgements

The microarray studies were performed at the Genomics Platform of the Institut de Recerca Vall d'Hebron (VHIR). We thank Fatima Nuñez (VHIR's Genomics Platform) for her help in designing the microarray experiment, Alex Sánchez and Ricardo González (VHIR's Statistics and Bioinformatics) for the statistical analysis of the microarray data, Alexis Rafols (CRG Histology Unit), Carmen Badosa, Juan D. Martinez and Eva Prats (CID Animal Facility) for technical support, and Mark Sefton for English editorial work.

Funding

This work was supported by grants from the Spanish Ministry of Economia, Industria y Competitividad (MINECO: SAF2013-46676-P and SAF2016-77971-R to M.L.A and BFU2013-44513 and BFU2016-76141 to S.L.), the Secretariat of Universities and Research-Generalitat de Catalunya (2014SGR674), and the Fundación Alicia Koplowitz. The group of S.L. acknowledges the support of the MINECO Centro de Excelencia Severo Ochoa programme and of the CERCA Programme (Generalitat de Catalunya). G.S-E. and M.P.S. acknowledge the support of the NIH National Institute of Neurological Disorders and Stroke of the National Institutes of Health (P01NS097197) and the Carlos III Institute of Health (ISCIII, PI13/00865, Fondo Europeo de Desarrollo Regional - FEDER "Away of making Europe", Spain). M.J.B. is supported by the CIBERER, an initiative of the ISCIII. J.A., E.B. and S.N. were supported by MINECO predoctoral fellowships (AP2012-3064 and BES2011-047472) and G.S-E. by a predoctoral fellowship from the Conchita Rábago Foundation.

Abbreviations

ASD	autism spectrum disorder
BrdU	bromodeoxyuridine
DD	developmental delay
DHS	*DYRK1A* haploinsufficiency syndrome
DS	Down syndrome
DYRK	dual-specificity tyrosine-regulated kinase
EEG	electroencephalogram
E/I	excitation/inhibition
GABA	γ-aminobutyric acid
GFP	green fluorescent protein
ID	intellectual disability
IUGR	intrauterine growth retardation
IVK	*in vitro* kinase
LDA	low-density array
LoF	loss-of function
SSC	somatosensory cortex
UsV	ultrasonic vocalization
WT	wild-type.

References

Alvarez M, Estivill X, de la Luna S, 2003 DYRK1A accumulates in splicing speckles through a novel targeting signal and induces speckle disassembly. J Cell Sci 116, 3099–3107. [PubMed: 12799418]

Aranda S, Laguna A, de la Luna S, 2011 DYRK family of protein kinases: evolutionary relationships, biochemical properties, and functional roles. FASEB J 25, 449–462. [PubMed: 21048044]

Arque G, Fotaki V, Fernandez D, Martinez de Lagran M, Arbones ML, Dierssen M, 2008 Impaired spatial learning strategies and novel object recognition in mice haploinsufficient for the dual specificity tyrosine-regulated kinase-1A (Dyrk1A). PLoS One 3, e2575. [PubMed: 18648535]

Barallobre MJ, Perier C, Bove J, Laguna A, Delabar JM, Vila M, Arbones ML, 2014 DYRK1A promotes dopaminergic neuron survival in the developing brain and in a mouse model of Parkinson's disease. Cell Death Dis 5, e1289. [PubMed: 24922073]

Becker W, Soppa U, Tejedor FJ, 2014 DYRK1A: a potential drug target for multiple Down syndrome neuropathologies. CNS Neurol Disord Drug Targets 13, 26–33. [PubMed: 24152332]

Benavides-Piccione R, Dierssen M, Ballesteros-Yanez I, Martinez de Lagran M, Arbones ML, Fotaki V, DeFelipe J, Elston GN, 2005 Alterations in the phenotype of neocortical pyramidal cells in the Dyrk1A+/− mouse. Neurobiol Dis 20, 115–122. [PubMed: 16137572]

Bozzi Y, Casarosa S, Caleo M, 2012 Epilepsy as a neurodevelopmental disorder. Front Psychiatry 3, 19. [PubMed: 22457654]

Bronicki LM, Redin C, Drunat S, Piton A, Lyons M, Passemard S, Baumann C, Faivre L, Thevenon J, Riviere JB, et al., 2015 Ten new cases further delineate the syndromic intellectual disability phenotype caused by mutations in DYRK1A. Eur J Hum Genet 23, 1482–1487. [PubMed: 25920557]

Courcet JB, Faivre L, Malzac P, Masurel-Paulet A, Lopez E, Callier P, Lambert L, Lemesle M, Thevenon J, Gigot N, et al., 2012 The DYRK1A gene is a cause of syndromic intellectual disability with severe microcephaly and epilepsy. J Med Genet 49, 731–736. [PubMed: 23099646]

Dang T, Duan WY, Yu B, Tong DL, Cheng C, Zhang YF, Wu W, Ye K, Zhang WX, Wu M, et al., 2018 Autism-associated Dyrk1a truncation mutants impair neuronal dendritic and spine growth and interfere with postnatal cortical development. Mol Psychiatry 23, 747–758. [PubMed: 28167836]

de la Torre-Ubieta L, Won H, Stein JL, Geschwind DH, 2016 Advancing the understanding of autism disease mechanisms through genetics. Nat Med 22, 345–361. [PubMed: 27050589]

De Rubeis S, He X, Goldberg AP, Poultney CS, Samocha K, Cicek AE, Kou Y, Liu L, Fromer M, Walker S, et al., 2014 Synaptic, transcriptional and chromatin genes disrupted in autism. Nature 515, 209–215. [PubMed: 25363760]

Deciphering Developmental Disorders S, 2015 Large-scale discovery of novel genetic causes of developmental disorders. Nature 519, 223–228. [PubMed: 25533962]

Di Vona C, Bezdan D, Islam AB, Salichs E, Lopez-Bigas N, Ossowski S, de la Luna S, 2015 Chromatin-wide profiling of DYRK1A reveals a role as a gene-specific RNA polymerase II CTD kinase. Mol Cell 57, 506–520. [PubMed: 25620562]

Earl RK, Turner TN, Mefford HC, Hudac CM, Gerdts J, Eichler EE, Bernier RA, 2017 Clinical phenotype of ASD-associated DYRK1A haploinsufficiency. Mol Autism 8, 54. [PubMed: 29034068]

Ernst C, 2016 Proliferation and differentiation deficits are a major convergence point for neurodevelopmental disorders. Trends Neurosci 39, 290–299. [PubMed: 27032601]

Evers JM, Laskowski RA, Bertolli M, Clayton-Smith J, Deshpande C, Eason J, Elmslie F, Flinter F, Gardiner C, Hurst JA, et al., 2017 Structural analysis of pathogenic mutations in the DYRK1A gene in patients with developmental disorders. Hum Mol Genet 26, 519–526. [PubMed: 28053047]

Florio M, Huttner WB, 2014 Neural progenitors, neurogenesis and the evolution of the neocortex. Development 141, 2182–2194. [PubMed: 24866113]

Fotaki V, Dierssen M, Alcantara S, Martinez S, Marti E, Casas C, Visa J, Soriano E, Estivill X, Arbones ML, 2002 Dyrk1A haploinsufficiency affects viability and causes developmental delay and abnormal brain morphology in mice. Mol Cell Biol 22, 6636–6647. [PubMed: 12192061]

Fotaki V, Martinez De Lagran M, Estivill X, Arbones M, Dierssen M, 2004 Haploinsufficiency of Dyrk1A in mice leads to specific alterations in the development and regulation of motor activity. Behav Neurosci 118, 815–821. [PubMed: 15301607]

Garcia-Cabrero AM, Marinas A, Guerrero R, de Cordoba SR, Serratosa JM, Sanchez MP, 2012 Laforin and malin deletions in mice produce similar neurologic impairments. J Neuropathol Exp Neurol 71, 413–421. [PubMed: 22487859]

Geschwind DH, 2009 Advances in autism. Annu Rev Med 60, 367–380. [PubMed: 19630577]

Golden CE, Buxbaum JD, De Rubeis S, 2018 Disrupted circuits in mouse models of autism spectrum disorder and intellectual disability. Curr Opin Neurobiol 48, 106–112. [PubMed: 29222989]

Guedj F, Pereira PL, Najas S, Barallobre MJ, Chabert C, Souchet B, Sebrie C, Verney C, Herault Y, Arbones M, et al., 2012 DYRK1A: a master regulatory protein controlling brain growth. Neurobiol Dis 46, 190–203. [PubMed: 22293606]

Guimera J, Casas C, Pucharcos C, Solans A, Domenech A, Planas AM, Ashley J, Lovett M, Estivill X, Pritchard MA, 1996 A human homologue of Drosophila minibrain (MNB) is expressed in the neuronal regions affected in Down syndrome and maps to the critical region. Hum Mol Genet 5, 1305–1310. [PubMed: 8872470]

Himpel S, Panzer P, Eirmbter K, Czajkowska H, Sayed M, Packman LC, Blundell T, Kentrup H, Grotzinger J, Joost HG, et al., 2001 Identification of the autophosphorylation sites and characterization of their effects in the protein kinase DYRK1A. Biochem J 359, 497–505. [PubMed: 11672423]

Himpel S, Tegge W, Frank R, Leder S, Joost HG, Becker W, 2000 Specificity determinants of substrate recognition by the protein kinase DYRK1A. J Biol Chem 275, 2431–2438. [PubMed: 10644696]

Huguet G, Ey E, Bourgeron T, 2013 The genetic landscapes of autism spectrum disorders. Annu Rev Genomics Hum Genet 14, 191–213. [PubMed: 23875794]

Jabaudon D, 2017 Fate and freedom in developing neocortical circuits. Nat Commun 8, 16042. [PubMed: 28671189]

Ji J, Lee H, Argiropoulos B, Dorrani N, Mann J, Martinez-Agosto JA, Gomez-Ospina N, Gallant N, Bernstein JA, Hudgins L, et al., 2015 DYRK1A haploinsufficiency causes a new recognizable syndrome with microcephaly, intellectual disability, speech impairment, and distinct facies. Eur J Hum Genet 23, 1473–1481. [PubMed: 25944381]

Kannan N, Neuwald AF, 2004 Evolutionary constraints associated with functional specificity of the CMGC protein kinases MAPK, CDK, GSK, SRPK, DYRK, and CK2alpha. Protein Sci 13, 2059–2077. [PubMed: 15273306]

Kii I, Sumida Y, Goto T, Sonamoto R, Okuno Y, Yoshida S, Kato-Sumida T, Koike Y, Abe M, Nonaka Y, et al., 2016 Selective inhibition of the kinase DYRK1A by targeting its folding process. Nat Commun 7, 11391. [PubMed: 27102360]

Kim OH, Cho HJ, Han E, Hong TI, Ariyasiri K, Choi JH, Hwang KS, Jeong YM, Yang SY, Yu K, et al., 2017 Zebrafish knockout of Down syndrome gene, DYRK1A, shows social impairments relevant to autism. Mol Autism 8, 50. [PubMed: 29021890]

Kriegstein A, Alvarez-Buylla A, 2009 The glial nature of embryonic and adult neural stem cells. Annu Rev Neurosci 32, 149–184. [PubMed: 19555289]

Landrum MJ, Lee JM, Benson M, Brown G, Chao C, Chitipiralla S, Gu B, Hart J, Hoffman D, Hoover J, et al., 2016 ClinVar: public archive of interpretations of clinically relevant variants. Nucleic Acids Res 44, D862–868. [PubMed: 26582918]

Lee E, Lee J, Kim E, 2017 Excitation/nhibition imbalance in animal models of autism spectrum disorders. Biol Psychiatry 81, 838–847. [PubMed: 27450033]

Li M, Cui Z, Niu Y, Liu B, Fan W, Yu D, Deng J, 2010 Synaptogenesis in the developing mouse visual cortex. Brain Res Bull 81, 107–113. [PubMed: 19751806]

Lochhead PA, Sibbet G, Morrice N, Cleghon V, 2005 Activation-loop autophosphorylation is mediated by a novel transitional intermediate form of DYRKs. Cell 121, 925–936. [PubMed: 15960979]

Lord C, Bishop SL, 2015 Recent advances in autism research as reflected in DSM-5 criteria for autism spectrum disorder. Annu Rev Clin Psychol 11, 53–70. [PubMed: 25581244]

Luco SM, Pohl D, Sell E, Wagner JD, Dyment DA, Daoud H, 2016 Case report of novel DYRK1A mutations in 2 individuals with syndromic intellectual disability and a review of the literature. BMC Med Genet 17, 15. [PubMed: 26922654]

Luttjohann A, Fabene PF, van Luijtelaar G, 2009 A revised Racine's scale for PTZ-induced seizures in rats. Physiol Behav 98, 579–586. [PubMed: 19772866]

Markram H, Toledo-Rodriguez M, Wang Y, Gupta A, Silberberg G, Wu C, 2004 Interneurons of the neocortical inhibitory system. Nat Rev Neurosci 5, 793–807. [PubMed: 15378039]

Martinez de Lagran M, Benavides-Piccione R, Ballesteros-Yanez I, Calvo M, Morales M, Fillat C, Defelipe J, Ramakers GJ, Dierssen M, 2012 Dyrk1A influences neuronal morphogenesis through regulation of cytoskeletal dynamics in mammalian cortical neurons. Cereb Cortex 22, 2867–2877. [PubMed: 22215728]

Miller MW, 1995 Relationship of the time of origin and death of neurons in rat somatosensory cortex: barrel versus septal cortex and projection versus local circuit neurons. J Comp Neurol 355, 6–14. [PubMed: 7636014]

Moller RS, Kubart S, Hoeltzenbein M, Heye B, Vogel I, Hansen CP, Menzel C, Ullmann R, Tommerup N, Ropers HH, et al., 2008 Truncation of the Down syndrome candidate gene DYRK1A in two unrelated patients with microcephaly. Am J Hum Genet 82, 1165–1170. [PubMed: 18405873]

Molyneaux BJ, Arlotta P, Menezes JR, Macklis JD, 2007 Neuronal subtype specification in the cerebral cortex. Nat Rev Neurosci 8, 427–437. [PubMed: 17514196]

Najas S, Arranz J, Lochhead PA, Ashford AL, Oxley D, Delabar JM, Cook SJ, Barallobre MJ, Arbones ML, 2015 DYRK1A-mediated Cyclin D1 degradation in neural stem cells contributes to the neurogenic cortical defects in Down syndrome. EBioMedicine 2, 120–134. [PubMed: 26137553]

O'Roak BJ, Vives L, Fu W, Egertson JD, Stanaway IB, Phelps IG, Carvill G, Kumar A, Lee C, Ankenman K, et al., 2012 Multiplex targeted sequencing identifies recurrently mutated genes in autism spectrum disorders. Science 338, 1619–1622. [PubMed: 23160955]

Ori-McKenney KM, McKenney RJ, Huang HH, Li T, Meltzer S, Jan LY, Vale RD, Wiita AP, Jan YN, 2016 Phosphorylation of beta-tubulin by the Down syndrome kinase, Minibrain/DYRK1A, regulates microtubule dynamics and dendrite morphogenesis. Neuron 90, 551–563. [PubMed: 27112495]

Packer A, 2016 Neocortical neurogenesis and the etiology of autism spectrum disorder. Neurosci Biobehav Rev 64, 185–195. [PubMed: 26949225]

Park JH, Jung MS, Kim YS, Song WJ, Chung SH, 2012 Phosphorylation of Munc18–1 by Dyrk1A regulates its interaction with Syntaxin 1 and X11alpha. J Neurochem 122, 1081–1091. [PubMed: 22765017]

Posey JE, Rosenfeld JA, James RA, Bainbridge M, Niu Z, Wang X, Dhar S, Wiszniewski W, Akdemir ZH, Gambin T, et al., 2016 Molecular diagnostic experience of whole-exome sequencing in adult patients. Genet Med 18, 678–685. [PubMed: 26633545]

Raveau M, Shimohata A, Amano K, Miyamoto H, Yamakawa K, 2018 DYRK1A-haploinsufficiency in mice causes autistic-like features and febrile seizures. Neurobiol Dis 110, 180–191. [PubMed: 29223763]

Ruaud L, Mignot C, Guet A, Ohl C, Nava C, Heron D, Keren B, Depienne C, Benoit V, Maystadt I, et al., 2015 DYRK1A mutations in two unrelated patients. Eur J Med Genet 58, 168–174. [PubMed: 25641759]

Rubenstein JL, 2010 Three hypotheses for developmental defects that may underlie some forms of autism spectrum disorder. Curr Opin Neurol 23, 118–123. [PubMed: 20087182]

Somogyi P, Tamas G, Lujan R, Buhl EH, 1998 Salient features of synaptic organisation in the cerebral cortex. Brain Res Brain Res Rev 26, 113–135. [PubMed: 9651498]

Souchet B, Guedj F, Sahun I, Duchon A, Daubigney F, Badel A, Yanagawa Y, Barallobre MJ, Dierssen M, Yu E, et al., 2014 Excitation/inhibition balance and learning are modified by Dyrk1a gene dosage. Neurobiol Dis 69, 65–75. [PubMed: 24801365]

Soundararajan M, Roos AK, Savitsky P, Filippakopoulos P, Kettenbach AN, Olsen JV, Gerber SA, Eswaran J, Knapp S, Elkins JM, 2013 Structures of Down syndrome kinases, DYRKs, reveal mechanisms of kinase activation and substrate recognition. Structure 21, 986–996. [PubMed: 23665168]

Stessman HA, Xiong B, Coe BP, Wang T, Hoekzema K, Fenckova M, Kvarnung M, Gerdts J, Trinh S, Cosemans N, et al., 2017 Targeted sequencing identifies 91 neurodevelopmental-disorder risk genes with autism and developmental-disability biases. Nat Genet 49, 515–526. [PubMed: 28191889]

Sztainberg Y, Zoghbi HY, 2016 Lessons learned from studying syndromic autism spectrum disorders. Nat Neurosci 19, 1408–1417. [PubMed: 27786181]

Tejedor F, Zhu XR, Kaltenbach E, Ackermann A, Baumann A, Canal I, Heisenberg M, Fischbach KF, Pongs O, 1995 minibrain: a new protein kinase family involved in postembryonic neurogenesis in Drosophila. Neuron 14, 287–301. [PubMed: 7857639]

Tejedor FJ, Hammerle B, 2011 MNB/DYRK1A as a multiple regulator of neuronal development. FEBS J 278, 223–235. [PubMed: 21156027]

Telley L, Govindan S, Prados J, Stevant I, Nef S, Dermitzakis E, Dayer A, Jabaudon D, 2016 Sequential transcriptional waves direct the differentiation of newborn neurons in the mouse neocortex. Science 351, 1443–1446. [PubMed: 26940868]

Trujillano D, Bertoli-Avella AM, Kumar Kandaswamy K, Weiss ME, Koster J, Marais A, Paknia O, Schroder R, Garcia-Aznar JM, Werber M, et al., 2017 Clinical exome sequencing: results from 2819 samples reflecting 1000 families. Eur J Hum Genet 25, 176–182. [PubMed: 27848944]

van Bon BW, Coe BP, Bernier R, Green C, Gerdts J, Witherspoon K, Kleefstra T, Willemsen MH, Kumar R, Bosco P, et al., 2016 Disruptive de novo mutations of DYRK1A lead to a syndromic form of autism and ID. Mol Psychiatry 21, 126–132. [PubMed: 25707398]

van Bon BW, Hoischen A, Hehir-Kwa J, de Brouwer AP, Ruivenkamp C, Gijsbers AC, Marcelis CL, de Leeuw N, Veltman JA, Brunner HG, et al., 2011 Intragenic deletion in DYRK1A leads to mental retardation and primary microcephaly. Clin Genet 79, 296–299. [PubMed: 21294719]

Wang T, Guo H, Xiong B, Stessman HA, Wu H, Coe BP, Turner TN, Liu Y, Zhao W, Hoekzema K, et al., 2016 De novo genic mutations among a Chinese autism spectrum disorder cohort. Nat Commun 7, 13316. [PubMed: 27824329]

Widowati EW, Ernst S, Hausmann R, Muller-Newen G, Becker W, 2018 Functional characterization of DYRK1A missense variants associated with a syndromic form of intellectual deficiency and autism. Biol Open 7.

Zhang Y, Kong W, Gao Y, Liu X, Gao K, Xie H, Wu Y, Zhang Y, Wang J, Gao F, et al., 2015 Gene mutation analysis in 253 Chinese children with unexplained epilepsy and intellectual/developmental disabilities. PLoS One 10, e0141782. [PubMed: 26544041]

Rump P, Jazayeri O, van Dijk-Bos KK, Johansson LF, van Essen AJ, Verheij JB, Veenstra-Knol HE, Redeker EJ, Mannens MM, Swertz MA, et al. 2016 Whole-exome sequencing is a powerful approach for establishing the etiological diagnosis in patients with intellectual disability and microcephaly. BMC Med Genomics 9, 7.

Highlights:

- Lack of kinase activity for *DYRK1A* missense mutations in DYRK1A haploinsufficiency syndrome
- Stereotyped behavior and epileptic activity in haploinsufficient *Dyrk1a*$^{+/-}$ mutant mice
- Alterations in neuron and synapse densities in the neocortex of *Dyrk1a*$^{+/-}$ mice
- Alterations in neurogenesis and transcriptomic profiles in the *Dyrk1a*$^{+/-}$ developing cortex

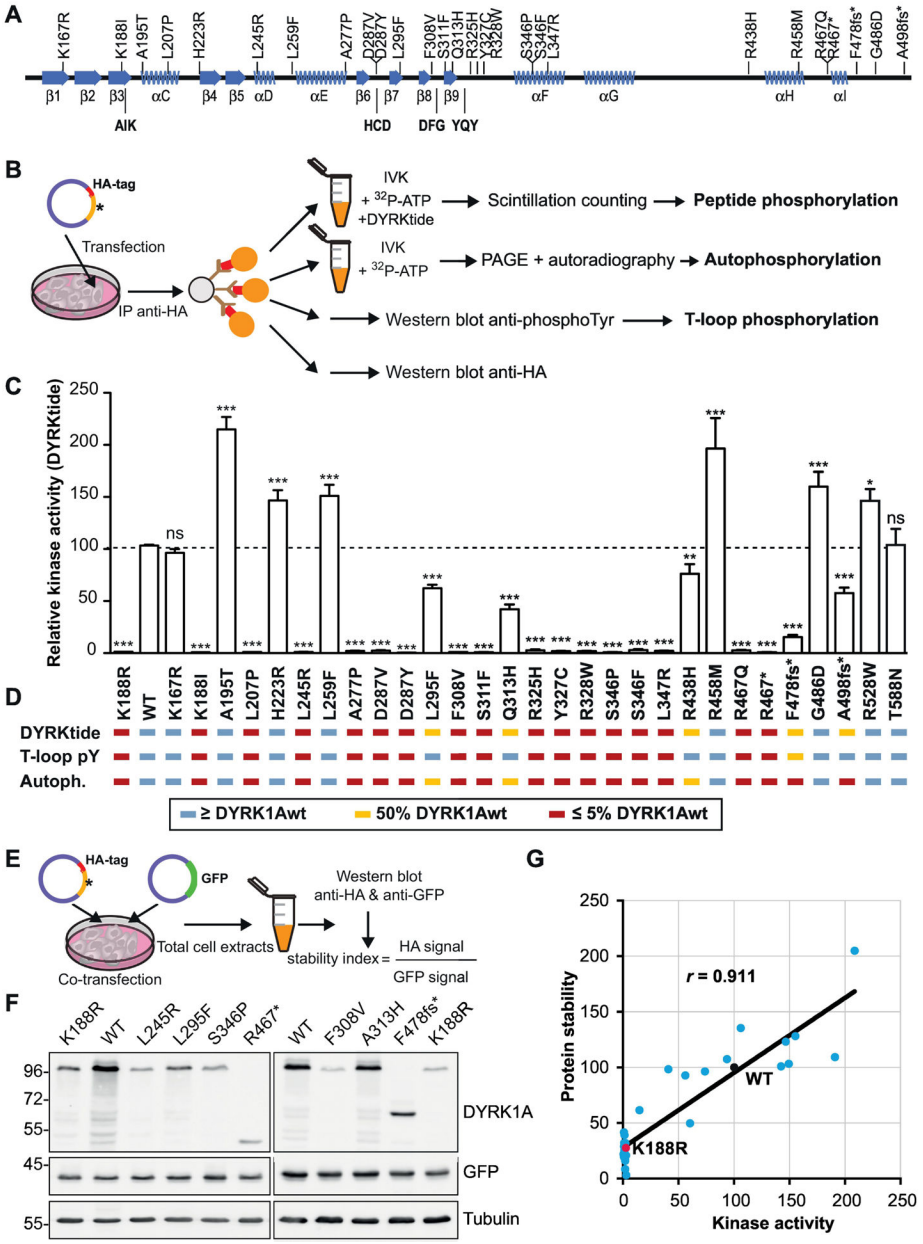

Fig. 1. *DYRK1A* missense mutations affect DYRK1A kinase activity, auto-phosphorylation and protein stability.

(A) Representation of the secondary protein structure of the DYRK1A catalytic domain, indicating the location of the mutants used in this study: AIK, HCD, DFG and YQY correspond to key functional elements (Kannan and Neuwald, 2004). (B) Experimental procedure followed to analyze the parameters summarized in (C) and (D). (C) The graph represents the ability of the mutants to phosphorylate the DYRKtide peptide, with the WT kinase activity arbitrarily set as 100. The catalytically inactive mutant K188R was also included in the assay (n=3 independent experiments; mean±SEM; ***$p < 0.001$, ns=not significant, unpaired 2-tailed Mann-Whitney's test). (D) Summary of the mutants' activity measured as the substrate phosphorylation, auto-phosphorylation and T-loop auto-

phosphorylation (see Supplementary Fig. 1B and C). (E, F) Scheme of the assay used to assess the impact of the mutations on protein accumulation (E). A representative experiment is shown (F; see also Supplementary Fig. 1C for quantification). (G) Correlation analysis of the activity and stability of the DYRK1A mutants. The WT protein and the kinase-inactive K188R mutant are indicated as black and red dots, respectively (Pearson's correlation, $r = 0.9211$; $p < 0.0001$).

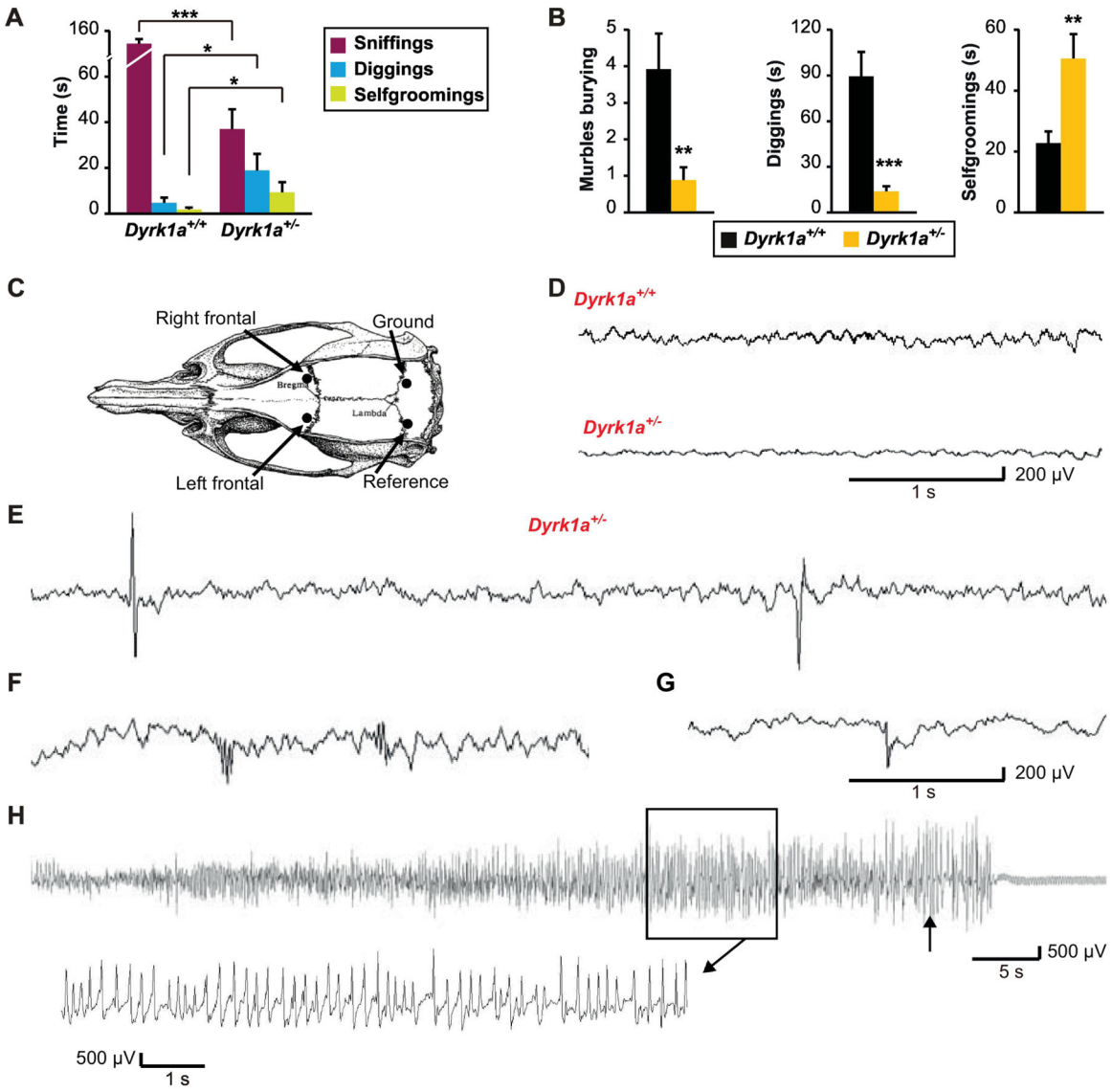

Fig. 2. *Dyrk1a*$^{+/-}$ mice display social deficits, repetitive behavior and epileptic activity.

(A) Social interaction test. Time spent by adult mice on social interactions (sniffing) and repetitive behavior (digging and self-grooming). (B) Marble-burying test in which the number of buried marbles, and the time spent by adult mice digging and on self-grooming was recorded over 20 min (n=12-15 mice each genotype: *$p < 0.05$, **$p < 0.01$, ***$p < 0.001$, Student's *t*-test). (C) Schematic drawing of a mouse skull indicating the electrode placement for EEG recordings. (D) Fragments of representative EEG recordings of the basal activity in *Dyrk1a*$^{+/+}$ and *Dyrk1a*$^{+/-}$ mice. (E-G) Representative EEG recordings of *Dyrk1a* $^{+/-}$ mice showing the spikes (E), polyspikes (F) and spike-wave discharges (G). (H) EEG recording of a spontaneous generalized tonic-clonic seizure lasting 74 s in a *Dyrk1a*$^{+/-}$ mouse (see also Supplementary Movie), with a 10 s amplified portion (black square) displaying spike-wave activity at a frequency of 4-5 Hz. The arrow indicates the beginning of the clonic phase.

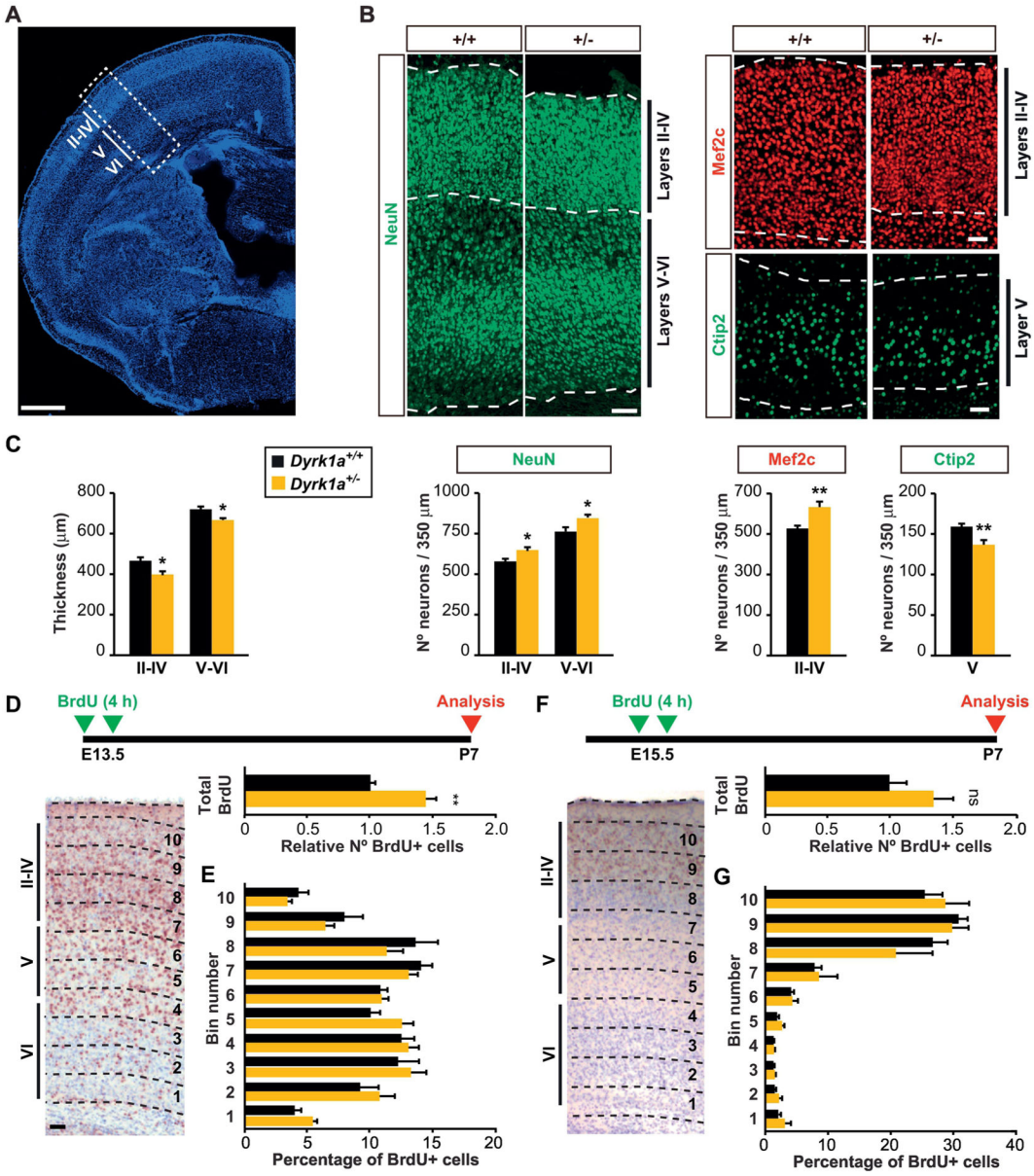

Fig. 3. *Dyrk1a*$^{+/-}$ mice show altered numbers of excitatory neurons in the postnatal neocortex.

(A) Coronal brain section from a P7 *Dyrk1a*$^{+/+}$ mouse stained with Hoechst indicating the position of the neocortical layers II to VI. Quantification in the somatosensory cortex (SSC, white dashed rectangle). (B) Representative images of *Dyrk1a*$^{+/+}$ (+/+) and *Dyrk1a*$^{+/-}$ (+/−) sections immunolabeled for NeuN, Mef2c or Citp2. (C) Histograms showing the thickness and number of neurons positive for the markers indicated in a 350 µm wide column of the external (layers II-IV) and internal (layers V-VI) layers of the neocortex (n=4-5 animals each genotype). (D-G) Schedule of the BrdU-labeling protocol to estimate neuron production in E13.5 (D) and E15.5 (F) embryos and representative images of *Dyrk1a*$^{+/+}$ sections immunolabeled for BrdU (brown signal) and the nuclei stained with Nissl. Histograms represent the total number of BrdU^{+} cells in *Dyrk1a*$^{+/-}$ animals relative to that in *Dyrk1a*$^{+/+}$ animals arbitrarily set as 1 (D-F), and the distribution of these cells in 10 equal bins,

represented as the percentage of $BrdU^+$ cells in each bin (E, G) ($BrdU^+$ cells at E13.5, n=7-9 animals each genotype; $BrdU^+$ cells at E15.5, n=5-6 animals each genotype). ns= not significant, *$p < 0.05$, **$p < 0.01$, Student's *t*-test. Bars = 100 μm (A) and 50 μm (B and D).

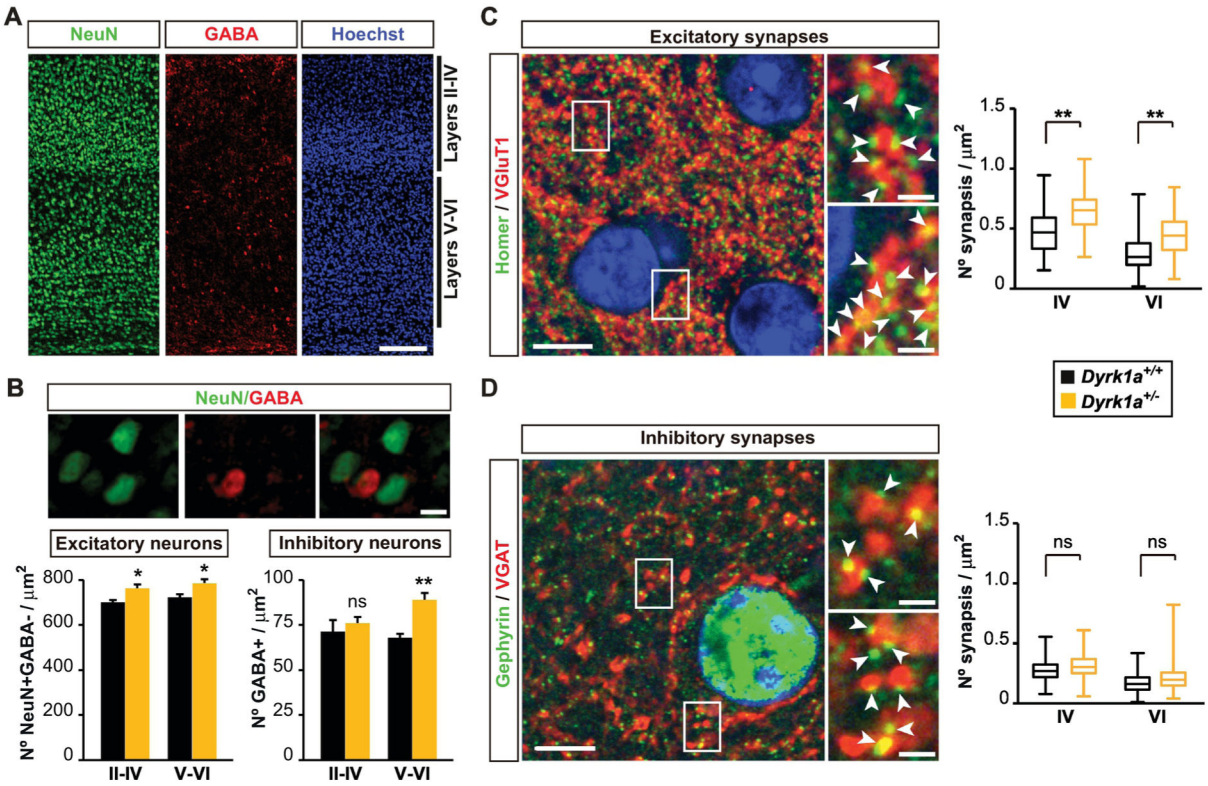

Fig. 4. Adult *Dyrk1a*$^{+/-}$ mice have a higher density of cortical neurons and synapses.

(A) Representative images of the SSC from a *Dyrk1a*$^{+/+}$ mouse section immunolabeled for NeuN and GABA, and counterstained with Hoechst nuclear dye. (B) Images showing NeuN^{+} and GABA^{+} neurons in the SSC, and histograms with the quantification of NeuN^{+}/GABA^{-} (excitatory) and GABA^{+} (inhibitory) neurons in the external (layers II-IV) and internal (layers V-VI) layers of a 350 µm wide column of the SSC (n=4 animals each genotype; ns= not significant, *$p < 0.05$, **$p < 0.01$, Student's *t*-test). (C, D) Representative confocal images of the SSC from a *Dyrk1a*$^{+/+}$ mouse immunolabeled for VGluT1 and Homer (C), or for VGAT and Gephyrin (D), with the nuclei labeled with DAPI (blue). White rectangles indicate the area magnified in the images on the right. The white arrowheads point to interactions between presynaptic and postsynaptic markers. Box plots show the synapse densities between the first and third quartiles, the line in the boxes corresponding to the median synapse density (see Supplementary Fig. 3 for the automatic quantification of synapses). Excitatory synapses, layer IV (*Dyrk1a*$^{+/+}$, n=639; *Dyrk1a*$^{+/-}$, n=661) and layer VI (*Dyrk1a*$^{+/+}$, n=639; *Dyrk1a*$^{+/-}$, n=643). Inhibitory synapses, layer IV (*Dyrk1a*$^{+/+}$, n=601; *Dyrk1a*$^{+/-}$, n=539) and layer VI (*Dyrk1a*$^{+/+}$, n=616; *Dyrk1a*$^{+/-}$, n=535) (6 animals per genotype; **$p < 0.01$, ns=not significant, nested one-way ANOVA). Bars = 200 µm (A), 10 µm (B), and 5 µm and 1 µm (left and right photographs respectively in C, D).

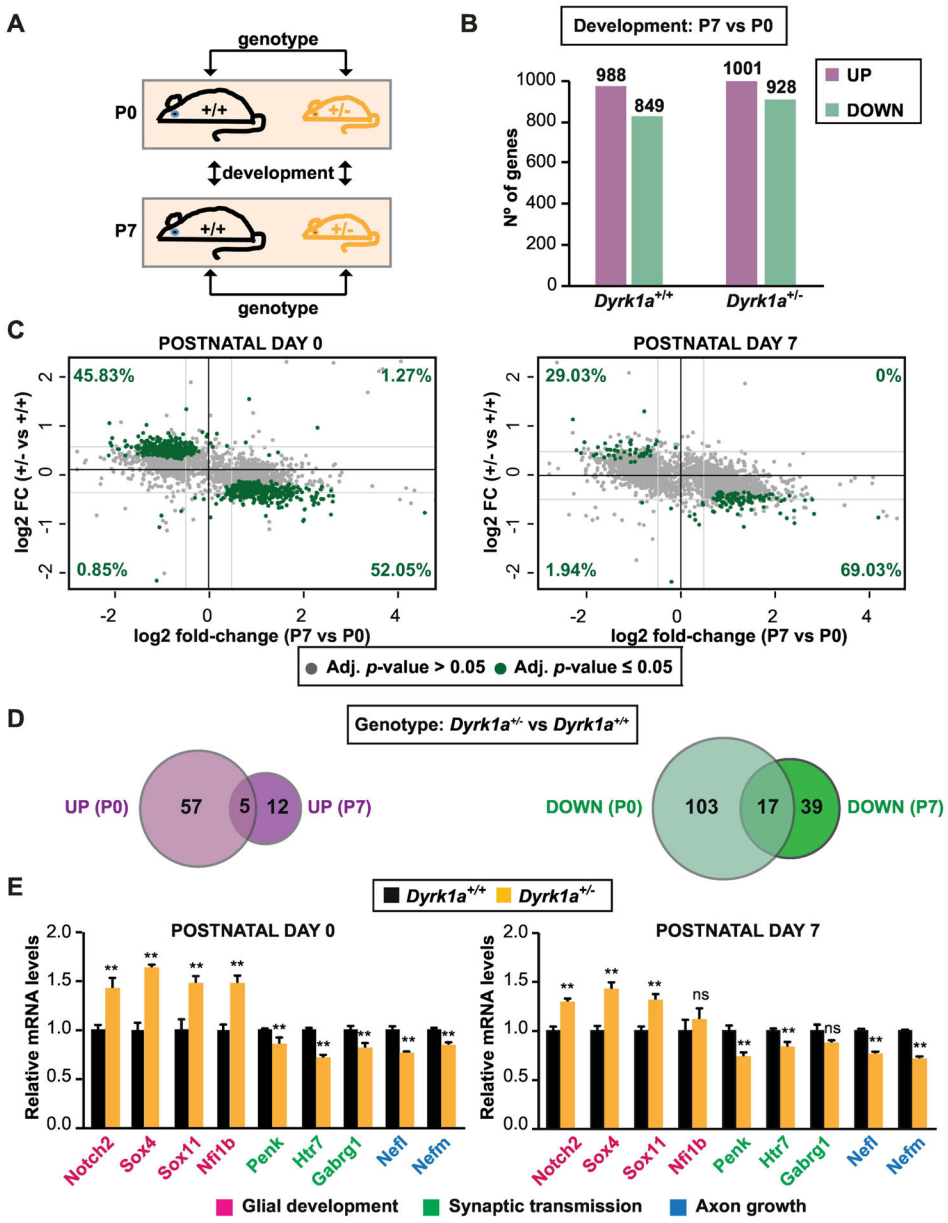

Fig. 5. Transcriptome alterations in the neocortex of postnatal *Dyrk1a*$^{+/-}$ mice.

(A) Schematic representation of the comparisons performed to identify differentially expressed genes during development or between genotypes (n=4 animals each condition). (B) Transcriptional changes in the P7 and P0 cortex from *Dyrk1a*$^{+/+}$ or *Dyrk1a*$^{+/-}$ mice (adj. $p \leq 0.05$; $-1.4 \leq FC \geq 1.4$). (C) Dot plots represent the changes in gene expression between genotypes (+/− *vs* +/+) at P0 and P7, and between the developmental stages (P7 *vs* P0) in the WT samples (+/+). Each dot represents a gene probe: green dots indicate probes with significant changes between genotypes (adjusted *p*-value <0.05); grey dots genes with no significant change. The numbers in green correspond to the percentage of green dots in each quadrant. Light grey lines indicate the log2 fold-change equal to ± 0.4. (D) The Venn diagrams show the genes up-regulated or down-regulated in comparisons of *Dyrk1a*$^{+/-}$ with *Dyrk1a*$^{+/+}$ mice at the two developmental time points studied, with the overlap indicating

genes altered at both P0 and P7 (adj. $p \leq 0.05$; $-1.4 \leq FC \geq 1.4$). (E) Validation by RT-qPCR of selected genes with altered expression in *Dyrk1a*$^{+/-}$ animals. The graphs represent the mRNA expression relative to that in WT animals arbitrarily set as 1. RT-qPCR was used for *Nfi1b*, *Penk, Htr7, Nefl* and *Nefm* (n=4-9 animals each condition), and LDA for *Gabrg1, Notch2*, *Sox4* and *Sox11* (n=4 animals each condition; ns=not significant, $*p < 0.05$, Student's *t*-test).

Table 1.

Mutations analyzed in this study

Mutation	ClinVar[a]	Reference	Catalytic activity[b]	Clinical traits[c]
K167R	-	De Rubeis et al., 2014	+	No information available
K188I	SCV000206791	Ji et al., 2015	−	IUGR; global DD; microcephaly; ID; seizures
A195T	-	Dang et al., 2018	+	Global DD; mild ID with particular impairments in language; complex partial epilepsy with epileptic encephalopathy
L207P	-	Decipher et al., 2015	−	IUGR; global DD; microcephaly; delayed speech and language development
H223R	SCV000620751	-	+	No information available
L245R	SCV000206792 SCV000807304	Ji et al,. 2015	−	IUGR; global DD; microcephaly; ID; severe speech delay
L259F	-	Decipher et al., 2015; Dang et al., 2018	+	No information available
A277P	SCV000571206	Decipher et al., 2015	−	Global DD; postnatal microcephaly
D287V	SCV000598121	Decipher et al., 2015	−	IUGR; microcephaly; specific learning disability
D287Y	-	Zhang et al., 2015	−	Severe ID/DD; generalized tonic-clonic seizures, febrile seizures
L295F	SCV000206793 SCV000321572	Ji et al., 2015	+/−	Mild global DD; microcephaly; severe speech delay
F308V	SCV000247240	-	−	No information available
S311F	SCV000586742 SCV000520979	Ruaud et al., 2015	−	Small stature; ID; microcephaly; epilepsy
Q313H	-	De Rubeis et al., 2014	+/−	No information available
R325H	SCV000574147	-	−	No information available
Y327C	SCV000599256	-	−	No information available
R328W	SCV000492371	Stessman et al., 2017	−	No information available
S346F	SCV000712522	-	−	No information available
S346P	SCV000196060	Decipher et al., 2015;Bronicki et al., 2015	−	Microcephaly; ID; absent or delayed speech development; seizures
L347R	-	Trujillano et al., 2017	−	Global DD; microcephaly; ID; seizures
R438H	-	Wang et al., 2016	+	No information available
R458M	-	Dang et al., 2018	+	No information available
R467Q	SCV000245477 SCV000534701	Decipher et al., 2015; Posey et al., 2016	−	Developmental regression; primary microcephaly; ID
R467*	SCV000206787 SCV000245476 SCV000618033	Ji et al., 2015; Posey et al., 2016	−	Global DD; moderate ID; severe speech delay; seizures
F478Sfs112*	-	Rump et al., 2016	−	Severe DD; low birth weight; brachycephaly
G486D	SCV000747759	Dang et al., 2018	+	ASD, learning disorder and macrocephaly
A498Pfs93*	SCV000056592 SCV000494645	O'Roak et al., 2012	+/−	Global DD; microcephaly; speech delay; febrile and febrile seizures
R528W	SCV000594478	-	+	No information
T588N	SCV000196065	Bronicki et al., 2015	+	Microcephaly; ID; absent or delayed speech development; seizures

[a] ClinVar: www.ncbi.nlm.nih.gov/clinvar (Landrum et al., 2016).

[b], +, kinase activity ≤ wt; +/− kinase activity ≈50% wt; −, kinase activity below 5% wt.

[c], only selected traits are shown; more detailed information is included in Supplementary Table 1.

ASD, autism spectrum disorder; DD, developmental delay; ID, intellectual disability IUGR, intrauterine growth retardation.